

R. J. Chen · H. Otsu · V. Lapoux · S. Boissinot · H. Baba · A. Matta ·  
M. Kurata-Nishimura · E. Pollacco · Y. Blumenfeld · F. Flavigny · S. Franchoo ·  
N. Fukuda · P. Gangnant · F. Hammache · C. Houarner ·  
N. Inabe · D. Kameda · J. F. Libin · C. Louchart · M. Matsushita · T. Motobayashi · L. Nalpas ·  
E. Y. Nikolskii · A. Obertelli · T. Onishi · E. Rindel · P. Rosier · H. Sakurai ·  
F. Saillant · M. Takechi · S. Takeuchi · Y. Togano · K. Yoneda · A. Yoshida · K. Yoshida

## Proton Elastic Scattering of $^{23,25}\text{F}$

Received: 5 October 2012 / Accepted: 6 January 2013 / Published online: 29 January 2013  
© Springer-Verlag Wien 2013

**Abstract** Proton elastic scatterings of neutron-rich nuclei  $^{23}\text{F}$  and  $^{25}\text{F}$  have been measured for the first time at 289 and 298 MeV/nucleon, respectively, using the MUST2 silicon strip detector array and RIBF facility at RIKEN. The differential cross section of  $^{25}\text{F}$  was found to be smaller than the calculation with the global potential by Koning and Deraloche. The small cross section of  $^{25}\text{F}$  can be well reproduced by an optical model calculation with a shallow and long-tail potential.

### 1 Introduction

Nuclear structures of neutron-rich nuclei have attracted much attention because of their exotic nature, such as neutron halo and neutron skin [1]. Evidence for the halo structures has been obtained mainly from the measurements of the interaction cross section [2] and the momentum distribution of the projectile fragments [3]. However, elastic scattering could be useful to investigate the structure of halo.

Recently, experimental studies showed that the dripline of fluorine isotopes was located at least 6 neutrons farther than that of the oxygen isotopes [4], for which the inclusion of three-nucleon forces provided a microscopic explanation [5]. The  $^{25}\text{F}$  is critical for the study of nuclear structure because it is only one proton off the  $^{24}\text{O}_{16}$  doubly magic nucleus [6, 7]. Theoretically, the calculation of the nonlinear relativistic mean-field (RMF) theory predicts neutron halo in  $^{25}\text{F}$  [8]. Experimentally, a large interaction cross section [2] and a significant reduction in the width of the momentum distributions [3] are shown for  $^{25}\text{F}$ . However, the neutron halo in  $^{25}\text{F}$  is still unknown. Therefore, we analyzed the  $^{23,25}\text{F}(p,p)$  elastic scattering data in order to investigate the neutron halo structure in  $^{25}\text{F}$ .

---

Presented at the 20th International IUPAP Conference on Few-Body Problems in Physics, 20–25 August, 2012, Fukuoka, Japan.

---

R. J. Chen  
School of Physics and State Key Laboratory of Nuclear Physics and Technology, Peking University, Beijing 100871, China

R. J. Chen · H. Otsu (✉) · H. Baba · M. Kurata-Nishimura · N. Fukuda · N. Inabe · D. Kameda · M. Matsushita · T. Motobayashi ·  
E. Y. Nikolskii · T. Onishi · H. Sakurai · M. Takechi · S. Takeuchi · Y. Togano · K. Yoneda · A. Yoshida · K. Yoshida  
RIKEN Nishina Center, Hirosawa 2-1, Wako, Saitama 351-0198, Japan  
E-mail: otsu@ribf.riken.jp

V. Lapoux · S. Boissinot · E. Pollacco · F. Flavigny · C. Louchart · L. Nalpas · A. Obertelli  
CEA-Saclay, DSM/IRFU SPhN, F-91191 Gif sur Yvette Cedex, France

A. Matta · Y. Blumenfeld · S. Franchoo · F. Hammache · E. Rindel · P. Rosier  
Institut de Physique Nucleaire, IN2P3-CNRS, F-91406 Orsay, France

P. Gangnant · C. Houarner · J. F. Libin · F. Saillant  
GANIL CEA/DSM-CNRS/IN2P3, BP 55027, F-14076 Caen Cedex 5, France

## 2 Experiment

The experiment was performed at the RI-beam factory (RIBF) operated by the RIKEN Nishina Center and the Center for Nuclear Study, University of Tokyo. The secondary beams were produced by bombarding a 15-mm-thick rotating Be target with a  $^{48}\text{Ca}$  beam at 345 MeV/nucleon with an average intensity of  $\sim 120$  particle nA. The fragments were identified event-by-event by measuring the energy loss ( $\Delta E$ ), magnetic rigidity ( $B\rho$ ) and time-of-flight (TOF) using the standard beamline detectors in the second stage of BigRIPS [9]. The  $^{23}\text{F}$  and  $^{25}\text{F}$  beams were produced as contaminants of the  $^{22}\text{O}$  and  $^{24}\text{O}$  beams, respectively. The intensities of  $^{23}\text{F}$  and  $^{25}\text{F}$  secondary beams were  $\sim 9.6 \times 10^3$  (purity 23%) and 330 (purity 1.3%) cps, respectively. The profiles of the secondary beams were deduced by 3 sets of parallel plate avalanche counters (PPACs) [10], with position resolution of about 2.8 mm (FWHM). Inside the vacuum chamber at F8, a polypropylene  $(\text{CH}_2)_n$  foil with a thickness of  $2.7 \text{ mg/cm}^2$  was used for the measurement by setting it with  $45^\circ$  along to beam line and face to the left side of detector arrays. A carbon foil with a thickness of  $0.78 \text{ mg/cm}^2$  was used for subtracting the contribution of carbon in the  $(\text{CH}_2)_n$  foil. The energy and scattering angle of recoil protons were measured using 4 sets of MUST2 telescopes [11] which were located at 23 cm downstream of the target, covering an angular region from  $65^\circ$  to  $90^\circ$  in the laboratory frame. Protons were identified by measuring the energy loss and energy with the double-sided silicon strip detector (DSSD) and the CsI detector, respectively. For low-energy protons stopped inside the DSSD, the time-of-flight between the PPACs and DSSD was used for the particle identification.

## 3 Result

The  $^{23,25}\text{F}(p,p)$  and  $(p,p')$  reaction channels were identified by incident beams in BigRIPS coincident with outgoing heavy residuals in the ZeroDegree Spectrometer and protons in MUST2. Figure 1 (left) shows the scatter plot of the proton laboratory angle versus energy for  $^{25}\text{F}$ , where the solid line corresponds to the elastic scattering. Figure 1 (right) shows the resulting excitation energy spectrum. In order to subtract the carbon component, a constant shape distribution has been assumed for the carbon component since the excitation energy spectrum for the carbon target was structureless. We note that the result obtained by this method should include the contribution from the inelastic scattering to the low-energy bound excited states, due to the limited energy resolution ( $\sim 2.1 \text{ MeV}$  in FWHM). However, based on the DWBA prediction, it is expected to be negligible compared to the elastic scattering contribution. Finally, the differential cross sections for the  $^{23}\text{F}(p,p)$  and  $^{25}\text{F}(p,p)$  elastic scatterings are shown in the left and right panels of Fig. 2, respectively. The errors are statistical errors. The solid line represents the optical model calculation with the global potential parameters by Koning and Delaroche [12] (KD potential) using Fresco code [13]. From Fig. 2, we can see that the differential cross section of  $^{23}\text{F}$  can be well reproduced by the calculation, while the cross section of  $^{25}\text{F}$  is smaller than the calculation. This would be explained by the different nuclear structure of  $^{25}\text{F}$  from stable nuclei since the global KD potential parameters were obtained from the measurements of stable nuclei. The reduction of the cross section of  $^{25}\text{F}$  is considered to be due to the shielding effect by the neutron skin. In order to understand the reduction of cross section of  $^{25}\text{F}$ , we adjusted the parameters of the global KD potential. Firstly, we only adjusted the depth of the imaginary potential and tried to reproduce the experimental cross section. The result is shown by the dashed line and the new parameters are given as set 1 in Table 1. We found that we could

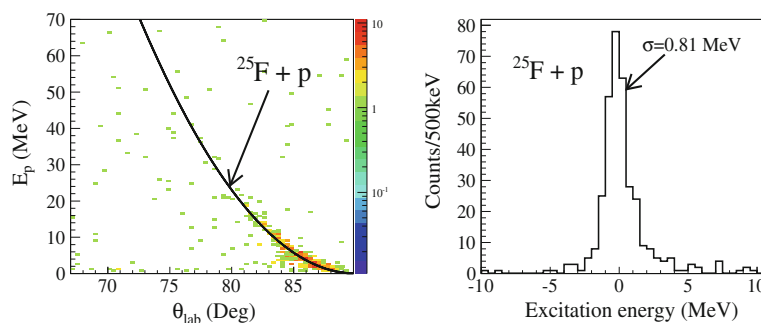


**Fig. 1** (left) Scatter plot of recoil proton energy versus scattering angle in the laboratory frame for  $^{25}\text{F}$ ; (right) Excitation energy spectrum for the proton scattering on  $^{25}\text{F}$

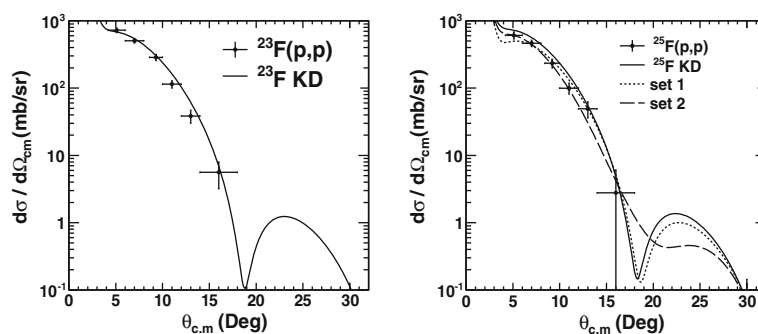


**Fig. 2** Differential cross sections for the  $^{23}\text{F}(p,p)$  (left) and  $^{25}\text{F}(p,p)$  (right) elastic scatterings

**Table 1** KD potential parameters

Name	$r_c$	$V_v$	$r_v$	$a_v$	$W_v$	$r_v$	$a_v$	$W_s$	$r_s$	$a_s$	$V_{s.o.}$	$W_{s.o.}$	$r_{s.o.}$	$a_{s.o.}$	$\chi^2/N$
KD	1.34	14.92	1.17	0.67	14.02	1.17	0.67	0.03	1.30	0.53	1.80	-2.40	0.96	0.59	
set 1	1.34	14.92	1.17	0.67	10.10	1.17	0.67	0.03	1.30	0.53	1.80	-2.40	0.96	0.59	2.00
set 2	1.34	14.92	1.17	0.67	4.42	1.80	0.54	0.03	1.30	0.53	1.80	-2.40	0.96	0.59	0.59

reproduce the experimental data only by reducing the depth of the imaginary potential. Secondly, we tried to adjust both the depth and shape of the imaginary potential. The result is shown by the long-dashed line and the new parameters are given as set 2 in Table 1. We found that a shallow potential with a longer tail could reproduce the result better. However, we need more sophisticated calculations in future analysis.

#### 4 Summary

The proton elastic scatterings of  $^{23}\text{F}$  and  $^{25}\text{F}$  were obtained at 289 and 298 MeV/nucleon, respectively. The cross section of  $^{25}\text{F}$  was found to be smaller than the optical model calculation with the KD potential and could be reproduced by a potential with a shallow and longer tail. More sophisticated calculations will be carried on.

**Acknowledgments** We would like to thank the accelerator staffs of RIKEN for their excellent operation. The author would like to thank China Scholarship Council (CSC) and RIKEN Nishina Center for financial support.

#### References

1. Tanihata, I.: Neutron halo nuclei. *J. Phys. G* **22**, 157 (1996)
2. Ozawa, A. et al.: Measurement of interaction cross sections for light neutron-rich at relativistic energies and determination of effective matter radii. *Nucl. Phys. A* **691**, 599 (2001)
3. Sauvan, E. et al.: One-neutron removal reactions on light neutron-rich nuclei. *Phys. Rev. C* **69**, 044603 (2004)
4. Sakurai, H. et al.: Evidence for particle stability of  $^{31}\text{F}$  and particle instability of  $^{25}\text{N}$  and  $^{28}\text{O}$ . *Phys. Lett. B* **448**, 180 (1999)
5. Otsuka, T. et al.: Three-body forces and the limit of oxygen isotopes. *Phys. Rev. Lett.* **105**, 032501 (2010)
6. Kanungo, R. et al.: One-neutron removal measurement reveals  $^{24}\text{O}$  as a new doubly magic nucleus. *Phys. Rev. Lett.* **102**, 152501 (2009)
7. Tshoo, K. et al.:  $N=16$  spherical shell closure in  $^{24}\text{O}$ . *Phys. Rev. Lett.* **109**, 022501 (2012)
8. Zhongzhou, Ren et al.: Relativistic mean-field study of odd- $A$  N and F isotopes. *J. Phys. G: Nucl. Part. Phys.* **22**, L1–L5 (1996)
9. Kubo, T.: In-flight RI beam separator BigRIPS at RIKEN and elsewhere in Japan. *Nucl. Instrum. Methods Phys. Res., Sect. B* **204**, 97 (2003)
10. Kumagai, H. et al.: Delay-line PPAC for high-energy light ions. *Nucl. Instr. and Meth. A* **470**, 562 (2001)
11. Pollacco, E. et al.: MUST2: A new generation array for direct reaction studies. *Eur. Phys. J. A* **25**, 287–288 (2005)
12. Koning, A.J., Delaroche, J.P.: Local and global nucleon optical models from 1 keV to 200 MeV. *Nucl. Phys. A* **713**, 231 (2003)
13. Thompson I., J.: Coupled reaction channels calculations in nuclear physics. *Comput. Phys. Rep.* **7**, 167 (1988)